Sedimentary Geology 350 (2017) 42–54

Contents lists available at ScienceDirect

Sedimentary Geology

journal homepage: www.elsevier.com/locate/sedgeo

High resolution ion microprobe investigation of the δ18O of carbonate cements (Jurassic, Paris Basin, France): New insights and pending questions

Benoit Vincent [a,*], Benjamin Brigaud [b], Laurent Emmanuel [c], Jean-Paul Loreau [d]

[a] Cambridge Carbonates Ltd, 1 rue de varoux, 21120 Marey sur Tille, France
[b] GEOPS, Univ. Paris-Sud, Université Paris Saclay, Rue du Belvédère, Bât. 504, 91405 Orsay cedex, France
[c] Sorbonne Universités – UPMC Univ. Paris 06, Institut des Sciences de la Terre de Paris, ISTeP UMR CNRS 7193, 4, place Jussieu, F-75005, Paris, France
[d] UMR 6282 Biogéosciences, Univ. Bourgogne Franche-Comté, CNRS, 6 Bd Gabriel, 21000, Dijon, France

ARTICLE INFO

Article history:
Received 13 November 2016
Received in revised form 25 January 2017
Accepted 27 January 2017
Available online 2 February 2017

Editor: Dr. B. Jones

Keywords:
SIMS
Carbonate
Diagenesis
$\delta^{18}O$
Heterogeneity

ABSTRACT

The scope of this work is to investigate, at a high resolution, the oxygen isotope composition ($\delta^{18}O_{carb}$) of diagenetic products (synsedimentary and burial calcite cements) in shallow-marine carbonates. SIMS (Secondary Ion Mass Spectrometry) microprobe analyses were performed on thin sections from Oxfordian and Kimmeridgian Formations of the eastern Paris Basin and compared to data obtained on the same diagenetic products by conventional mass spectrometry (acid digestion). Hereby obtained, $\delta^{18}O$ are similar, but the SIMS dataset displays a larger range of values.

The isotopic zonation obtained by SIMS transects through sequences of cements filling pores, reveals an (expected) isotopic depletion from older stage synsedimentary calcites to younger stage blocky calcites and that follows the CL (cathodoluminescence) zonation. SIMS analyses however show that synsedimentary cements precipitated in intra-skeletal pores, have heavier $\delta^{18}O$ than their inter-particle counterparts, with an offset of $+4‰_{V\text{-}PDB}$, despite similar petrographical characteristics. This difference is maintained in the $\delta^{18}O$ of the first stages of blocky calcite cements, intra-skeletal blocky calcites showing heavier $\delta^{18}O$ than the time equivalent and petrographically identical inter-particle calcites, with an offset of $+5‰_{V\text{-}PDB}$. These offsets are tentatively explained by the precipitation of cements under non-equilibrium conditions in intra-skeletal pores, where organic matter decay may have played a key role, acting notably on the pH.

The occurrence of isolated micro-diagenetic environments, co-existing at the thin section scale, is tentatively proposed as an explanation to these small scale and high amplitude $\delta^{18}O$ heterogeneities. These results may question the sampling strategy for future works. Microdrilling may miss the observed range of variation, but averaging the values may not necessarily lead to real misinterpretations if a critical selection of samples is performed, targeting potentially similar micro-diagenetic environments and avoiding potentially specific ones, *i.e.* closed intra-skeletal pores.

These results also definitely underscore the need for additional experiments to improve the reliability of SIMS, in order to develop the use of this very high resolution technique for carbonate diagenesis studies.

© 2017 Elsevier B.V. All rights reserved.

1. Introduction

Considerable variation is commonly reported in the oxygen and carbon stable isotope composition of neritic carbonates (*e.g.* Morse and Mackenzie, 1990; Tucker and Wright, 1990). This spread in values reflects the variety of (1) the paleo-depositional settings and sedimentary processes, and (2) the diagenetic processes (cementation, replacement, recrystallisation) that affect neritic carbonates. This variation has been extensively investigated because C & O stable isotopes are crucial paleoenvironmental and/or paleohydrologial proxies used in several fields of research (paleoclimatology, hydrogeology, oil and gas exploration…; *e.g.* Veizer, 1983; Moore, 1989; Tucker and Wright, 1990; Hendry, 1993; Joachimsky, 1994; Jenkyns, 2010; Martin-Garin et al., 2010; Dera et al., 2011; Deville de Periere et al., 2011). During the last 30 years, the sampling techniques became more refined with the development of computer-guided microdrills coupled with microscopes (*e.g.* Dettman and Lohmann, 1995), laser ablation techniques (*e.g.* Smalley et al., 1989; Dickson et al., 1990), and SIMS (Secondary Ion microprobe Mass Spectrometry; *e.g.* Ireland, 1995), which require considerably smaller quantities of sample. The two first techniques are

* Corresponding author.
E-mail address: benoit@cambridgecarbonates.co.uk (B. Vincent).
URL: http://www.cambridgecarbonates.com (B. Vincent).

http://dx.doi.org/10.1016/j.sedgeo.2017.01.008
0037-0738/© 2017 Elsevier B.V. All rights reserved.

commonly used by carbonate sedimentologists, despite some technical limitations like a possible thermal fractionation during O stable isotope analysis with laser ablation for instance (*e.g.* Kyser, 1995). The SIMS technique has been used extensively recently, but mostly on crustal/mantle-related problematics and far less in sedimentological research (*e.g.* Rollion-Bard et al., 2003a, 2003b, 2008; Allison et al., 2007, 2010), to even almost not used in diagenetic studies (Cox et al., 2010).

In this paper SIMS ion microprobe was used to measure at a high spatial resolution the oxygen stable isotope signal ($\delta^{18}O_{carb}$) of diagenetic products (synsedimentary and burial calcite cements) of Oxfordian (159.4 Ma ± 3.6 to 154.1 Ma ± 3.2) and Kimmeridgian (154.1 Ma ± 3.2 to 150.7 Ma ± 3) shallow marine carbonates of the eastern Paris Basin. The main objective is to investigate the small scale $\delta^{18}O$ heterogeneities in these products – *e.g.* between the luminescence zones of an individual crystal, to try to define or at least to discuss their origin(s), and finally to address the relevance of these uncommonly small scale variations through by comparison with data obtained on the same products by a classical method (conventional mass spectrometry).

2. Geological setting

A borehole, HTM102 (described in detail in Vincent et al., 2007), drilled by the Andra (French National Agency for Radioactive Waste Management) was chosen as being representative of the regional Oxfordian to Kimmeridgian carbonate series of the eastern Paris Basin and served as a continuous record for observations and sampling (Fig. 1). An outcrop (Gudmont-Villiers section; Fig. 1B, C) was selected so that the stratigraphic interval of the study could be extended to include the clayey formations at the top of the Early Kimmeridgian.

2.1. Sedimentology and stratigraphy

Detailed facies descriptions and information on the sequence stratigraphic setting are available in several publications (Vincent, 2001; Vincent et al., 2007; Carpentier et al., 2007, 2010; Brigaud et al., 2014), but relevant data with regard to the present geochemical investigation are presented here. For most of the Late Jurassic, a carbonate

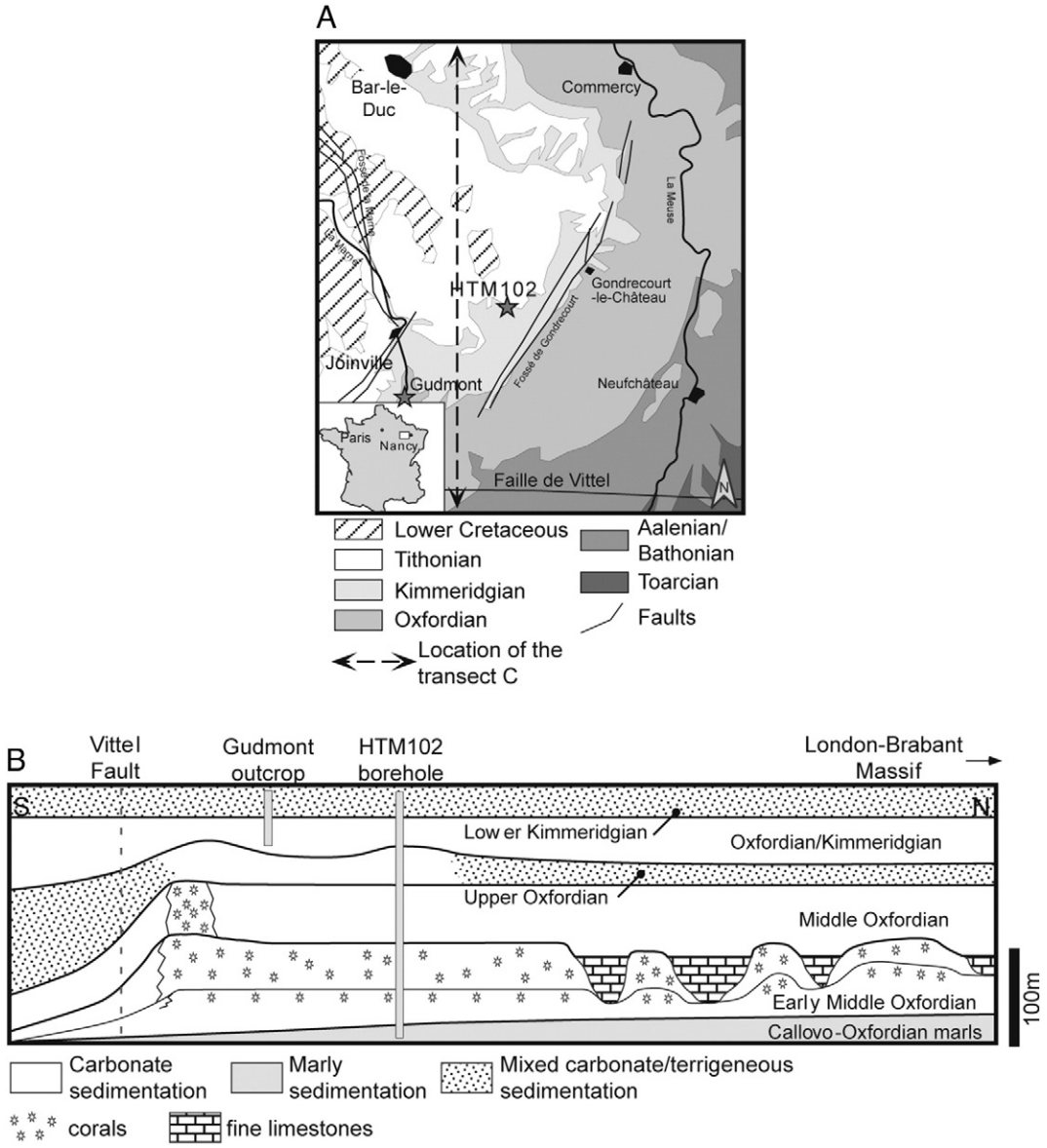

Fig. 1. A- Simplified geological map of the study area situating the HTM102 borehole and the Gudmont-Villiers outcrop (stars); B- Schematic North-South transect illustrating the evolution of the successive morphologies of the carbonate platform of Lorraine through Oxfordian and Kimmeridgian stages (after Humbert, 1971; Hilly and Haguenauer, 1979; Debrand-Passard et al., 1980; Vincent, 2001).

platform dipping southwards from the London-Brabant landmass developed over most of the eastern Paris Basin. It was bounded to the south by the Vittel fault (Fig. 1A). First a rimmed shelf formed during the Middle Oxfordian with highly diversified facies and prominent paleotopographic features resulting from the different growth rates of the underlying reefs of the Corallian groups, which formed above relatively homogeneous Callovian-Oxfordian marly homoclinal ramp deposits known as the "Woëvre clays" (Carpentier et al., 2010). All the negative topographic features were filled with fine micritic limestone during the Middle Oxfordian, and a shallow flat top platform extended between the London-Brabant landmass and the Vittel fault (Fig. 1B; Carpentier et al., 2010). In the Late Oxfordian, carbonate production was partly stopped by terrigenous input and mixed carbonate/terrigenous sedimentation occurred in a wide but shallow depression near this landmass. Carbonate sedimentation was confined to a narrow shoal in the southern part of the platform (Fig. 1B). With the onset of the Kimmeridgian, carbonate production resumed over the entire area. The Upper Oxfordian topography was progressively flattened and the platform was more open and exposed to fair-weather wave action. In the Early Kimmeridgian, there was renewed siliciclastic flux in the quiet-water sedimentation which was very homogeneous over the entire shelf (Fig. 1B). This input increased progressively to become dominant at the Early/Late Kimmeridgian boundary and the Late Kimmeridgian is characterized by a marl formation ("*Exogyra nana* marls").

2.2. Diagenesis

The paragenetic sequence comprises 3 early marine phases, 5 burial phases, and a phase of calcite dissolution for which timing is not firmly constrained, but likely late and linked to alteration by meteoric fluids during uplift. A brief petrographic description of the phases analyzed in this work is provided below, but the reader should refer to Vincent et al. (2007) or Carpentier et al. (2014) for further details.

Three types of early or syn-sedimentary cements of marine origin, all unclear and dirty (solid inclusions?) to different degree, are recognized: bladed and fibrous isopachous fringes, pendant fringes, and syntaxial sparry cements growing around echinoderm debris (mostly crinoids). Only the bladed isopachous fringes and the syntaxial sparry cements were analyzed. Under cathodoluminescence (CL), they display a mottled luminescence given by a general non-luminescence or blue intrinsic luminescence dotted with orange spots. Some more reddish spots, rarely observed, probably correspond to microdolomite rhombs. The fibrous cements always display a brighter luminescence than the bladed and syntaxial cements. All these morphological and luminescence characteristics indicate an actual non-ferroan Low Magnesium Calcite (LMC; uniform pink-red coloring) but suggest a former High Magnesium Calcite (HMC) initial mineralogy (*e.g.* Lohmann and Meyers, 1977; Aissaoui, 1988).

Three successive blocky calcite cements, labelled Bc1, Bc2, and Bc3, were observed, and were all analyzed in this study. For comparison, blocky calcites Bc1 and Bc2 are grouped and labelled Cal3 by Carpentier et al. (2014). Bc1 cements are mosaics of limpid spars and are well developed in the inter-particle and intra-particle primary pores. They also form syntaxially upon earlier synsedimentary syntaxial cements around echinoderm debris. These non-ferroan cements (uniform pink-red coloring) display concentric growth zones (Figs. 4, 5), indicating that the calcite was initially LMC and thus has not been recrystallized. Two zones are identifiable in Bc1 cements (Figs. 4, 5):

- Zone A: moderate orange luminescence with slightly darker and barely visible concentric stripes (brown/orange),
- Zone B: brown luminescence, again with slightly darker and barely visible concentric stripes.

The Bc2 cement displays a sector zoning with a mix of brown and orange stripes and fill biomolds and minor primary pores. There is no petrographic insight to clearly differentiate the timing of precipitation of Bc1 and Bc2, and they are grouped as a single phase in the paragenetic sequence.

The Bc3 last stage of cement corresponds to blocky, non-ferroan (pink-red coloring), LMC calcites, filling fractures throughout the stratigraphic column. Under CL these cements are non-luminescent to dull. Blocky cement Bc3 is labelled Cal4 by Carpentier et al. (2014).

3. Methods and techniques

The choice of features to be investigated by oxygen stable isotope analysis was based on a previously established paragenetic sequence (Vincent et al., 2007 their Figure 3). Sedimentary features such as brachiopod and oyster shells were analyzed by conventional mass spectrometry to provide data from which seawater temperatures were calculated. Diagenetic features included synsedimentary calcite cements, and burial calcite cements. These features whose size exceeded approximately 500 μm were sampled manually with a dentist microdrill (800 μm diameter), and this concerns only blocky cements. The dataset reveals a high variability of the oxygen isotope values, but a totally homogeneous rock-buffered carbon isotope signal in the various types of features (+2.6‰ ± 0.5 in Vincent et al., 2007). Therefore the present investigation focuses on the heterogeneity of the oxygen stable isotope signal with *in situ* SIMS analysis performed on thin sections.

3.1. Conventional mass spectrometry

Stable oxygen isotope analyses were carried out at the Laboratory ISTeP (Institut des Sciences de la Terre de Paris, UPMC, Paris, France). Powdered samples were reacted during 15 min with 100% H_3PO_4 acid under vacuum in an extraction line at 50 °C ("common acid bath"; Swart et al., 1991), and the resulting CO_2 was analyzed using a SIRA VG MM903 mass spectrometer. Oxygen isotope values ($\delta^{18}O$) are reported as per mil (‰) deviation in the isotope ratio ($^{18}O/^{16}O$) standardized to the Vienna Peedee belemnite - VPDB scale using an internal standard (Marceau marble: $\delta^{18}O = -1.83‰_{\text{V-PDB}} \pm 0.1‰$) calibrated against NBS-19, using classical methods (McCrea, 1950). Analytical reproducibility (1σ) on replicate analyses was 0.1‰ for $\delta^{18}O$.

3.2. SIMS in situ analyses

The *in situ* measurements were made on thin sections impregnated with blue-dyed epoxy and finely polished with diamond powder. Analyses were performed during two sessions with the SIMS Cameca IMS 1270, located at the CRPG laboratory in Nancy (France). Circular portions of the thin sections were extracted so as to be adapted to the apparatus, and gold coated prior to the analysis. Samples were sputtered with a 10 kV Cs^+ primary beam of 5 nA, focused on ~30-40 μm spots; the crater depth of the impact was <1 μm. In order to avoid potential interactions with the epoxy and/or dyes used for thin section preparation, analyses were, as far as possible, performed away from visible impregnated zones. Also, the width of the spots and the depth of the craters were small enough to minimize the risk of penetrating epoxy that would possibly exist in depth below the surface of the thin section. Secondary negative oxygen ions were accelerated at 10 kV and analyzed at a mass resolution of about 5000 using the circular focusing mode of the IMS 1270 and a transfer optic of 150 μm (Rollion-Bard et al., 2003a). Data collection was done over 15 cycles of 2 s each.

The instrumental fractionation was determined prior to each of the two sessions using a calcite crystal standard (MEX) analyzed conventionally with a value of 23.64‰$_{\text{SMOW}}$. The homogeneity of the standard was checked by multiple measurements along various profiles. The stability of the instrument was checked during each session by introducing 5 analyses on the standard every 2 h approximately. No apparent instrument drift was reported in either sessions.

The internal precision was calculated from the standard deviation (σ) of the 15 cycles in each analysis and was typically ±0.3‰$_{V\text{-}PDB}$. Reproducibility based on 10 repeated measurements of the standard was ±0.4‰$_{V\text{-}PDB}$. Long term reproducibility on the MEX calcite standard was studied by Rollion-Bard et al. (2003b).

All the isotopic values from calcites are given in permil deviation from the V-PDB standard (‰$_{V\text{-}PDB}$).

3.3. Electron Microprobe Compositional Maps

In order to investigate the trace/major element (Fe, Mn, Mg, and Sr) composition of the products analyzed with the SIMS, electron microprobe compositional maps were performed on two zones where relevant transects were acquired, after SIMS analysis on re-polished thin sections. Despite these maps providing interesting insights to the discussion, this is not a critical aspect of this work and the reader is kindly invited to refer to De Andrade et al. (2006) where details on the analytical protocol are provided. The maps produced in this study are semi-quantitative and do not provide absolute elemental compositions (there was no calibration against a standard). Comparison between calcite crystals are possible within one mapped zone but not between the two mapped zones.

4. Results

4.1. Oxygen Stable Isotope Compositions

The $\delta^{18}O$ values, including 93 SIMS data and 20 microdrilling-derived data, are distributed among two groups (Fig. 2; data in Appendix): (1) synsedimentary bladed isopachous and syntaxial cements, and (2) blocky calcite cements.

The $\delta^{18}O$ of synsedimentary cements range between −3.3‰ ± 2.7 and −3.8‰ ± 1.5 (Fig. 2). The $\delta^{18}O$ of the blocky calcite cements are clearly differentiated with a more negative signature (−7.9‰ ± 2.3). An ANOVA (Analysis Of Variance) performed on the blocky cement data set indicates that the mean isotopic compositions of the three families of blocky cements (Bc1, Bc2, and Bc3) are not significantly different ($p = 0.0723 > 0.05$; Vincent et al., 2007). In general, SIMS and microdrilling-derived data obtained on the same features are coherent (Fig. 2), although SIMS dataset display a larger spread in $\delta^{18}O$.

SIMS allows to obtain transects through cemented pores which illustrate the dynamics of progressive cementation in pores (*e.g.* Cox et al., 2010). Several transects were performed with two on the same thin section (Fig. 3), one in an inter-particle pore (Fig. 4), and the other in intra-particle, here intra-skeletal, pore (Fig. 5). The results reveal the complexity of the geochemical investigation at such a high resolution. First of all, the expected decrease of $\delta^{18}O$ from sedimentary elements (bioclasts) and early diagenetic cements to the burial cement does occur as in other case studies (*e.g.* Cox et al., 2010). Early synsedimentary or burial blocky cements, however can display significantly different $\delta^{18}O$ values at the thin section scale, illustrating co-existing distinct diagenetic micro-environments, which is discussed in detail later. Secondly, two very high oxygen isotope values, *i.e.* +5.4‰ and +8.2‰, were measured from the same bright orange luminescent thin CL stripe separating successive cements in two distinct transects in the same pore (Fig. 4). Compared to usual ranges for diagenetic calcite cements, especially in the Jurassic Formations of the Paris Basin and adjacent areas (*e.g.* Carpentier et al., 2014; Sellwood et al., 1989), these two values may appear anomalously high. As stated by Jimenez-Lopez et al. (2004), the occurrences of natural carbonates with unusually high $\delta^{18}O$ mostly remain unexplained, and a significant amount of new investigations would be necessary to confirm and then to find a cause for these two anomalous data.

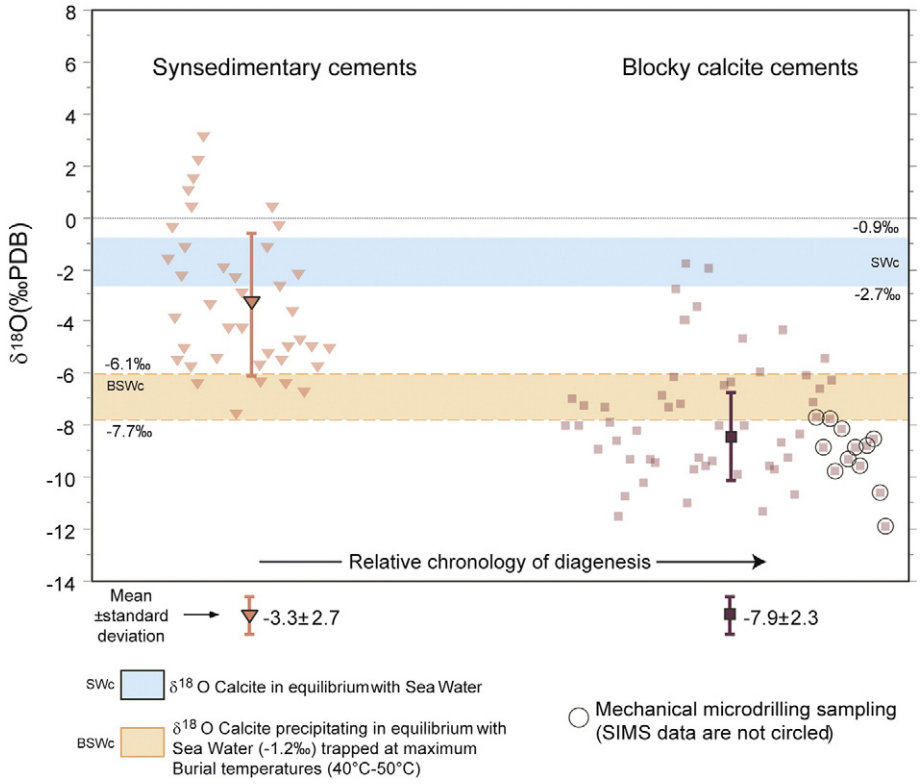

Fig. 2. $\delta^{18}O_{PDB}$ data (*in situ* SIMS measurements and microdrilled powders) of synsedimentary cements, and blocky calcite cements. Data are processed as ranges corresponding to mean plus or minus standard deviation for each product, but individual points are illustrated to better figure the range of variation. The ranges of (1) $\delta^{18}O$ of calcites in equilibrium with Upper Jurassic sea water, and (2) $\delta^{18}O$ of theoretical calcites which would have precipitated in equilibrium with the same sea water trapped and heated at maximum burial temperatures, are indicated as thermal constrains (see details in the text).

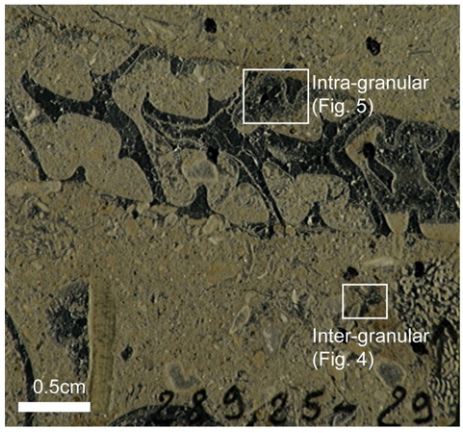

Fig. 3. Thin section photograph (HTM102–289.25-29) with the location of two key SIMS transects analyzed in detail in this work, *i.e.* in an inter-particle pore and an intra-gastropod pore.

5. Discussion

Discussing the genesis of diagenetic carbonates always necessitates to first constrain the thermal and burial history of the studied limestone.

5.1. Thermal Evolution of the Studied Carbonates

LMC brachiopods and oyster shells, known to be of potential use as paleoenvironmental proxies (*e.g.* Brand et al., 2003; Brigaud et al., 2008; Dhillon et al., 2015), were microdrilled and isotopically analyzed conventionally. A seawater isotopic composition of −1.2‰$_{SMOW}$ (Shackleton and Kennet, 1975; see discussion in Vincent et al., 2007, and Dera et al., 2011) was chosen for temperature calculation from the O'Neil et al. (1969) fractionation equation. The LMC shells provided a range of $\delta^{18}O$ of −1.8‰ ± 0.9, giving initial temperatures of the Oxfordian and Kimmeridgian seawaters of 18.6 °C ± 4.1. This seawater paleotemperature reconstruction is consistent with the paleotemperature range (17–24 °C) inferred from 264 $\delta^{18}O$ analyses on Late Jurassic oyster shells coming from the same area (Brigaud et al., 2008)

On the other hand, the maximum burial temperatures reached by the studied limestone never exceeded 40 to 50 °C until present, as indicated by multiple analyses (Clermonte et al., 1998; Elie et al., 1999; Landais and Elie, 1999; Blaise et al., 2014). The isotopic compositions of calcites precipitating in equilibrium from unmodified interstitial marine water buried to temperatures between 40 °C and 50 °C should fall between −6.1‰ and −7.7‰.

5.2. Diagenetic Micro-environments and Intracrystalline $\delta^{18}O$ variability

Initial oxygen isotope marine values are expected for the isopachous bladed and syntaxial synsedimentary cements analyzed with the SIMS

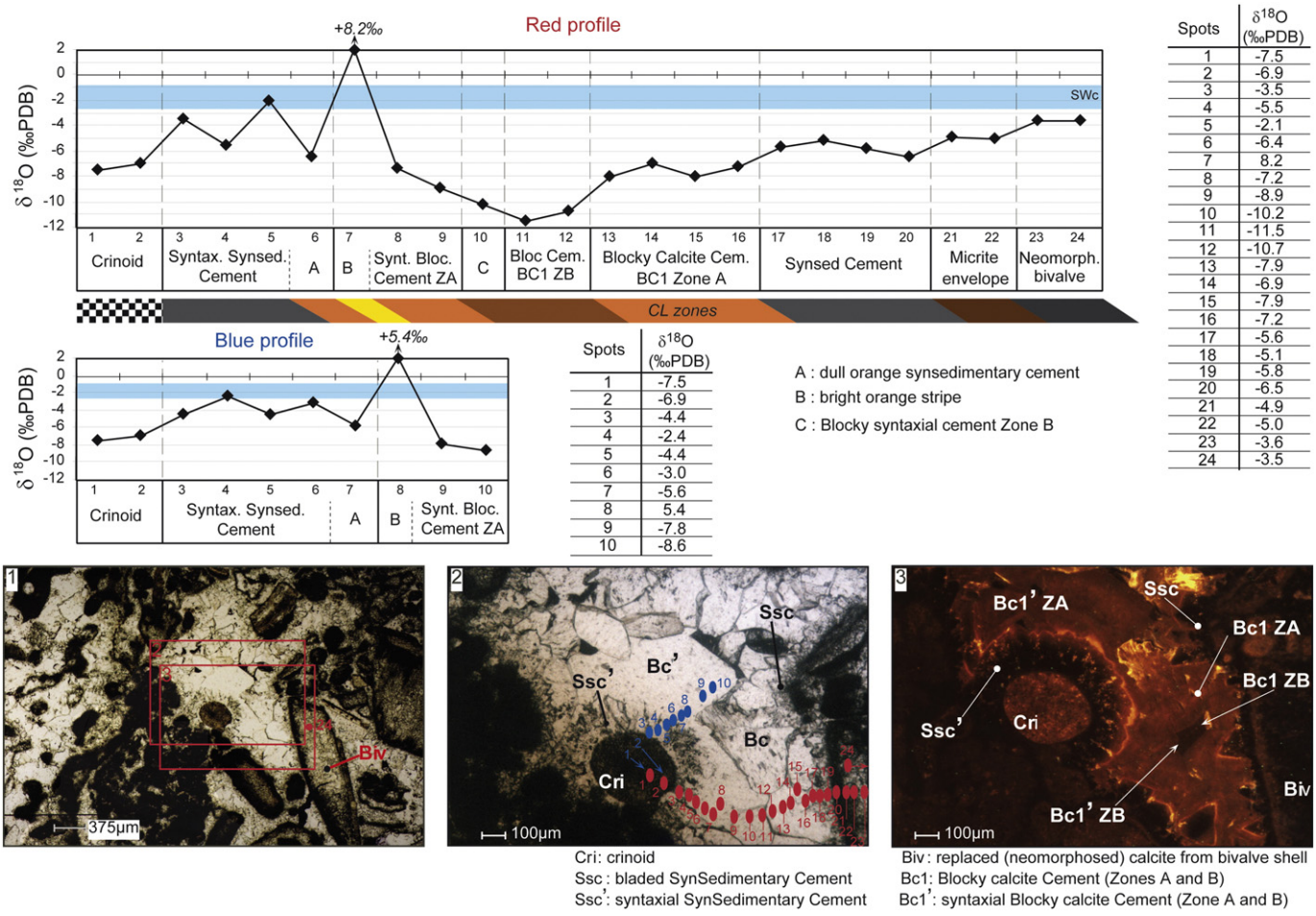

Spots	δ18O (‰PDB)
1	-7.5
2	-6.9
3	-4.4
4	-2.4
5	-4.4
6	-3.0
7	-5.6
8	5.4
9	-7.8
10	-8.6

Spots	δ18O (‰PDB)
1	-7.5
2	-6.9
3	-3.5
4	-5.5
5	-2.1
6	-6.4
7	8.2
8	-7.2
9	-8.9
10	-10.2
11	-11.5
12	-10.7
13	-7.9
14	-6.9
15	-7.9
16	-7.2
17	-5.6
18	-5.1
19	-5.8
20	-6.5
21	-4.9
22	-5.0
23	-3.6
24	-3.5

Fig. 4. Detailed SIMS $\delta^{18}O$ transects performed through the inter-particle pore. The $\delta^{18}O$ symmetrically decrease from the grains to the center of the pore recording the evolution of fluid composition-temperature during diagenesis and pore occlusion (see detailed discussion in the text; SWc indicates calcites in equilibrium with sea water, see Fig. 2). Parallel transects (blue and red) display identical relative and absolute $\delta^{18}O$ variations. Photo 1: large view of the sediment. Photo 2: Focus on the inter-particle pore with the position of the two analyzed transects and the position of each SIMS analytical point. Photo 3: CL view allowing to follow the evolution of $\delta^{18}O$ with CL zonation. (For interpretation of the references to colour in this figure legend, the reader is referred to the web version of this article.)

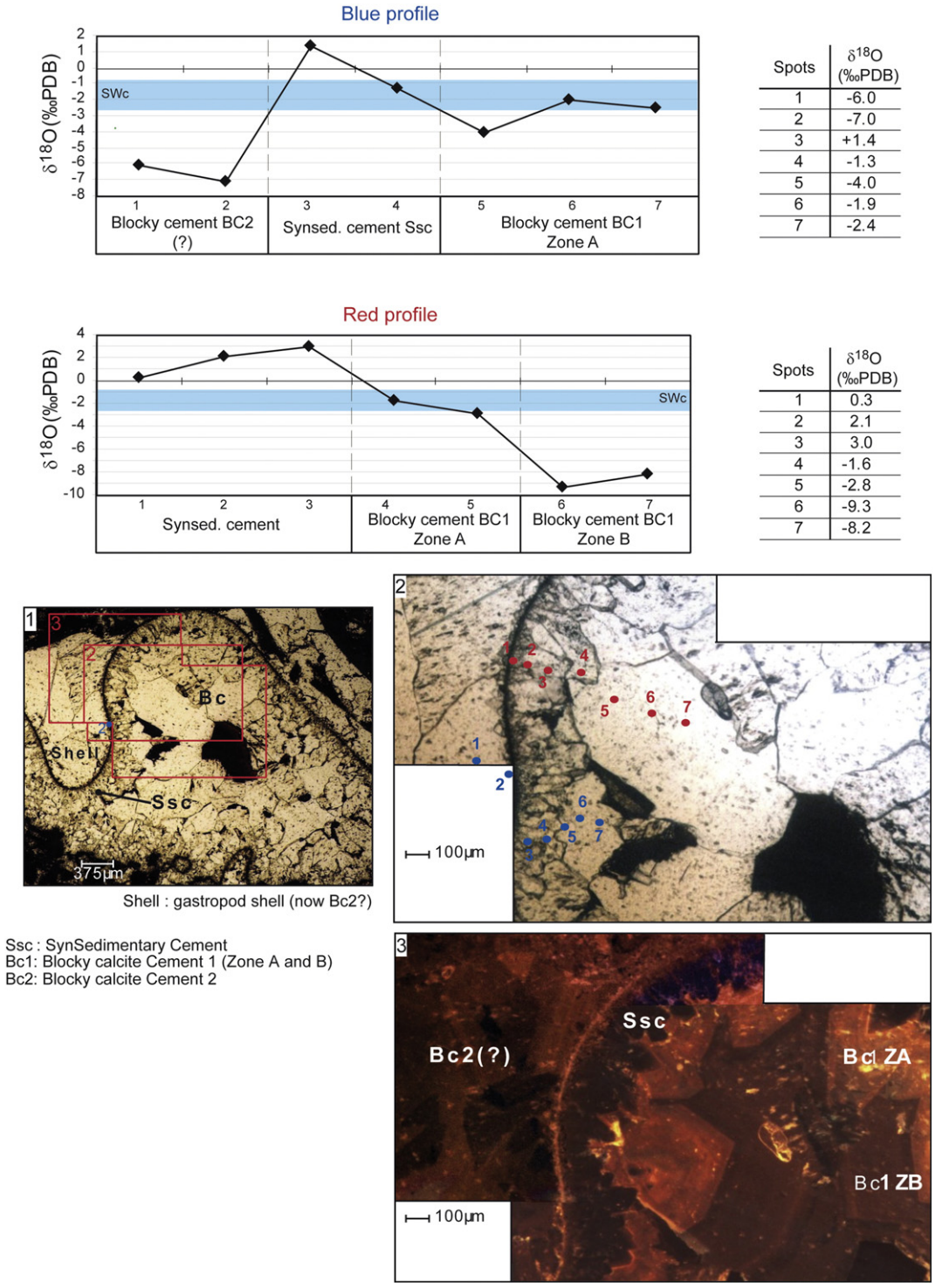

Spots	$\delta^{18}O$ (‰PDB)
1	-6.0
2	-7.0
3	+1.4
4	-1.3
5	-4.0
6	-1.9
7	-2.4

Spots	$\delta^{18}O$ (‰PDB)
1	0.3
2	2.1
3	3.0
4	-1.6
5	-2.8
6	-9.3
7	-8.2

Shell : gastropod shell (now Bc2?)

Ssc : SynSedimentary Cement
Bc1: Blocky calcite Cement 1 (Zone A and B)
Bc2: Blocky calcite Cement 2

Fig. 5. Detailed SIMS $\delta^{18}O$ transects performed through the intra-particle (gastropod) pore. The $\delta^{18}O$ also decrease towards the center of the pore like in the inter-particle counterpart, but absolute values for the same products, i.e. bladed synsedimentary cement and blocky calcite cement Bc1 Zones A and B, are systematically heavier (see detailed discussion in the text). Parallel transects (blue and red) display identical relative and absolute $\delta^{18}O$ variations. Photo 1: large view of the pore. Photo 2: Focus on the intra-particle pore with the position of the two analyzed transects and the position of each SIMS analytical point. Photo 3: CL view of photo 2 allowing to follow the evolution of $\delta^{18}O$ with CL zonation. (For interpretation of the references to colour in this figure legend, the reader is referred to the web version of this article.)

given that they precipitate immediately after deposition. However they display scattered compositions ($-3.3‰ \pm 2.7$) which generally lie between the range of marine values and the theoretical values of calcites precipitating from marine waters at maximum burial temperatures (Fig. 2). The general shift towards depleted $\delta^{18}O$ compositions of the synsedimentary cements is linked to the fact that they were certainly initially composed of HMC (see above). Although it is unknown at what stage in the diagenesis the HMC-LMC recrystallization occurred, this process could cause a shift in mean cement compositions towards more negative values. This can be achieved either through a thermal re-equilibration during burial, through the interaction of burial fluids with more negative $\delta^{18}O_{SMOW}$ than initial marine fluids during recrystallization, and/or through intergrowths of later burial cement among the fine primary structure of the cement (*e.g.* Frank and Lohmann, 1996).

Some of the data are, however, shifted to heavier values, and even positive (Fig. 2). In fact, the highest $\delta^{18}O$ compositions of bladed synsedimentary cements correspond to calcite fringes precipitated within closed intra-skeletal pores, such as gastropod chambers (Figs. 5, 6) or agglutinating foraminifera chambers (Fig. 7). Cements growing in open inter-particle pores display more classical marine or slightly depleted $\delta^{18}O$ values, and this phenomenon is even observed for the same synsedimentary bladed cement, within a single sample at thin section scale (Fig. 6). In this sample, where the SIMS full transects where performed, synsedimentary cementation likely occurred simultaneously in both pore-types.

Under equilibrium conditions, two parameters influence the $\delta^{18}O$ of a calcite: the $\delta^{18}O_{SMOW}$ of its parent fluids and the temperature of precipitation (*e.g.* Anderson and Arthur, 1983). The difference between the compositions of intra and inter-particle cements cannot be ascribed to a difference of temperature again, given that this phenomenon is observed for the same bladed synsedimentary cement, within a single sample (see above). Similarly, it is difficult to consider a strongly heterogeneous $\delta^{18}O$ composition of the pore fluids between intra- and inter-particle pores. Indeed, the heavier $\delta^{18}O$ of the intra-skeletal cements should illustrate heavier $\delta^{18}O$ of the parent fluids which may results either from (1) evaporation related fractionation, or (2) involvement of carbonates from dissolution of aragonite, aragonite being enriched in ^{18}O compared to coeval calcite (*e.g.* Morse and Mackenzie, 1990). Evaporation is easily ruled out since it may have concerned all interstitial fluids, whatever the pore type. The petrographic investigation demonstrated that aragonite moldic dissolution postdated synsedimentary cementation, thus that aragonite is not a likely source of carbonate for synsedimentary cements. Diagenetic HMC-LMC recrystallization cannot explain the differences of isotopic compositions observed between the intra and inter-particle products given that in both locations (1) both initial and present mineralogies are identical, and (2) the recrystallization processes involved are identical. Despite recrystallization is not necessarily uniform, this may only enhance or reduce these isotopic differences which seem of primary origin.

All the above discussion assumes a precipitation of the analyzed bladed synsedimentary cements under equilibrium conditions, whatever the pore type. This hypothesis is certainly true for the inter-particle pore, because cements grew slowly from a solution where isotopic equilibrium between dissolved carbonate species (HCO_3^-, CO_3^{2-}) and H_2O is attained (*e.g.* Dietzel et al., 2009). Indeed, considering the limited development of bladed synsedimentary cements in inter-particle pores (Figs. 7, 8), water renewal and oxygenation, key parameters favoring early marine cement growth (*e.g.* Dravis, 1979; De Wet et al., 2004; Christ et al., 2015), may have been limited in the sediments, facilitating isotopic equilibrium in the solution. Then, in inter-particle pores, bladed synsedimentary cements precipitated from carbonate ions with no kinetic effects in the solution.

Despite an even slower water renewal and possibly a lower oxygenation in the intra-skeletal pores, the latter display thicker synsedimentary bladed cements (Fig. 6) than the inter-particle pores. The closed intra-skeletal pores correspond to internal parts of ancient living organisms and were potentially rich in organic matter with regard to the open inter-particle pores. A variety of biochemical process(es) associated with microbial activity in the presence of organic matter and/or associated EPS (Extracellular Polymeric Substance), are known to promote carbonate precipitation in modern sediments, notably through their ability to increase the alkalinity of the depositional system (*e.g.* Riding, 2000; organomineralization *sensu* Dupraz et al., 2009). Their positive influence on the development of early carbonate cements has already been shown (Neumeier, 1998; Castanier et al., 1999), although in the geological record this mostly remains hypothetical. Identifying the influence of one or several of these existing processes is far beyond the scope of this work, but their occurrence within intra-skeletal pores is the most likely explanation for the difference of size of the synsedimentary rims. Microbial catalysis (*e.g.* Hendry, 1993) of dissolved carbonate species for sustained precipitation and faster growth rates of synsedimentary calcites may have hampered reaching an isotopic equilibrium in the solution of intra-skeletal pores. Indeed, several studies demonstrate that the growth rates of calcites directly

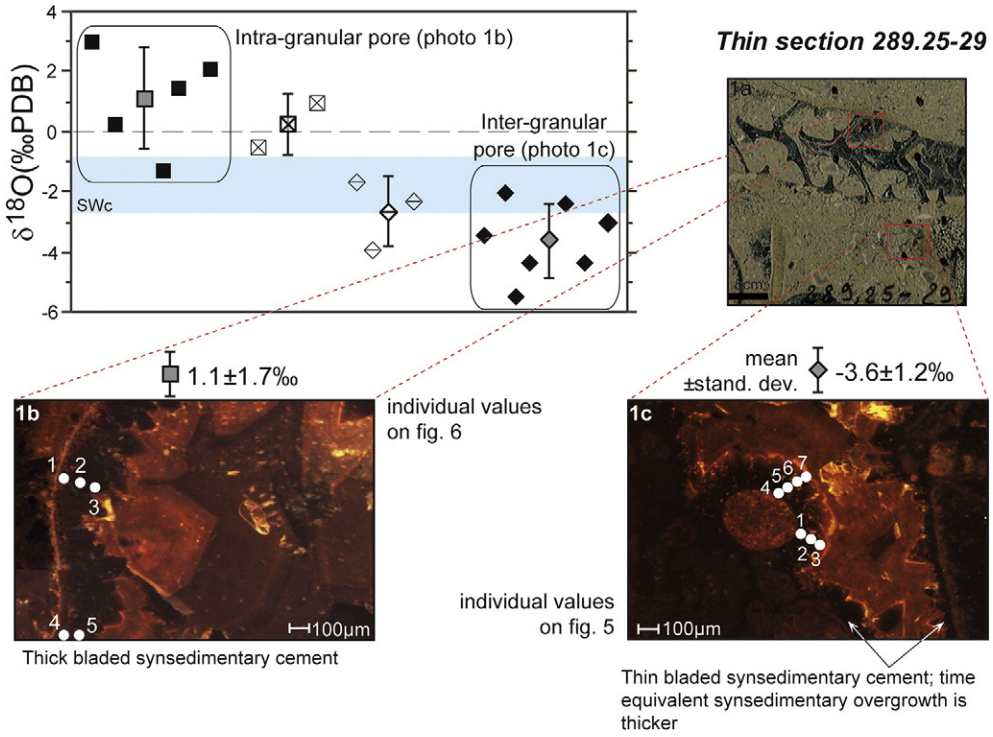

Fig. 6. Compared $\delta^{18}O_{PDB}$ of bladed synsedimentary cement in inter- and intra-particle pores of the same sample/thin section (HTM102/289.25–29). In the inter-particle pore, synsedimentary cement is poorly developed except as syntaxial overgrowth around echinoderm fragment and its $\delta^{18}O$ is lighter than the calcite in equilibrium with sea water. In the intra-particle pore, the synsedimentary cement is thick and its $\delta^{18}O$ is heavier than the than the calcite in equilibrium with sea water.

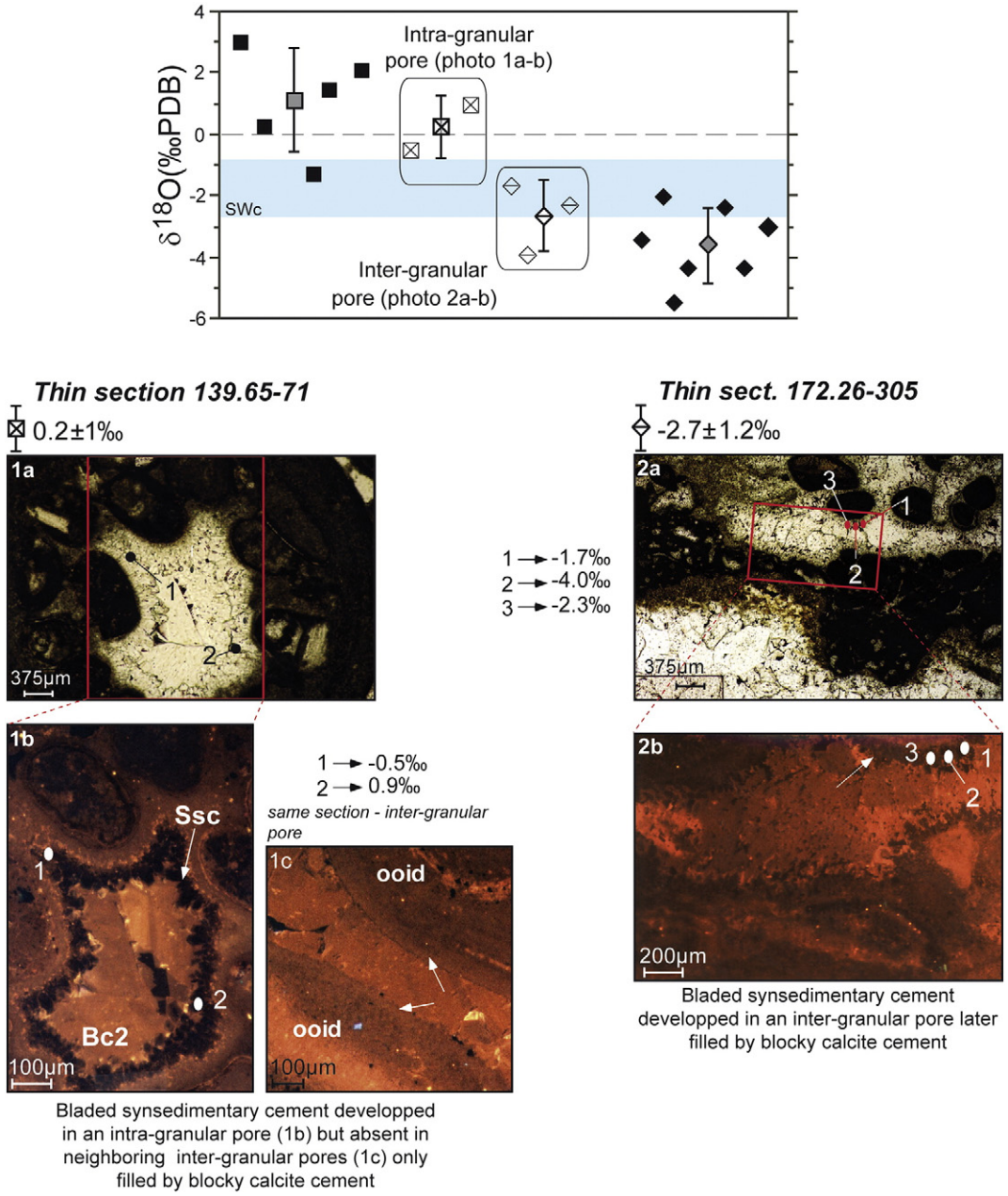

Fig. 7. $\delta^{18}O_{PDB}$ of bladed synsedimentary cement in inter- and intra-particle pores of other samples (HTM102/139.65–71; 172.26–305). Rims in intra-particle pore display heavier $\delta^{18}O$ than in inter-particle pore, where they are always thinner or even absent.

impact the fractionation factor between calcite and water ($\alpha_{calcite\text{-}water}$), leading to deviation from the classically admitted equilibrium values (Dietzel et al., 2009; Gabitov et al., 2012; Riechelmann et al., 2013). Therefore, in this kind of pores, oxygen isotopic fractionation between calcite and water may have been controlled by kinetic effects in the solution, and the pH may also have been then one important factor as demonstrated by Dietzel et al. (2009) from laboratory experiments on inorganically grown calcites. If some microbial processes are promoting carbonate precipitation, other processes such as degradation of organic matter through aerobic bacterial oxidation, or bacterial sulphate reduction, reversely inhibit carbonate growth and even can promote dissolution through acidification (*e.g.* Dupraz et al., 2009). Even if no petrographic evidence (such as framboidal pyrite) supports the past occurrence of bacterial sulphate reduction, some of the above processes likely occurred anyway in the intra-skeletal pores, lowering the pH of pore waters, before and in alternation with the processes promoting cement growth. Sass et al. (1991) showed that bacterial sulphate reduction leads to a slight $\delta^{18}O$ depletion of the resulting calcites, but Dietzel et al. (2009) demonstrate that $\alpha_{calcite\text{-}water}$ significantly increases with a decreasing pH. This influence of pH on the $\delta^{18}O$ of precipitating carbonates has also been emphasized for coral growth (Rollion-Bard et al., 2003b; Allison et al., 2010). Therefore, acidification of the medium through degradation of organic matter in intra-skeletal pores may be considered as one possible cause of the heavier $\delta^{18}O$ of the synsedimentary calcite cements, compared to the values of the same cements in inter-particle pores, and despite a similar marine parent fluid. It is worth to note that no evidence of dissolution of the substrate of the synsedimentary calcite cements were observed in the intra-skeletal pores on thin sections, but it is as well necessary to claim that a higher resolution petrographic investigation (involving SEM, Scanning Electron Microscope) may be necessary to properly identify such a phase.

A SIMS investigation of the carbon isotope signal, similar to the one realized in this work for $\delta^{18}O$, would nevertheless be necessary in order

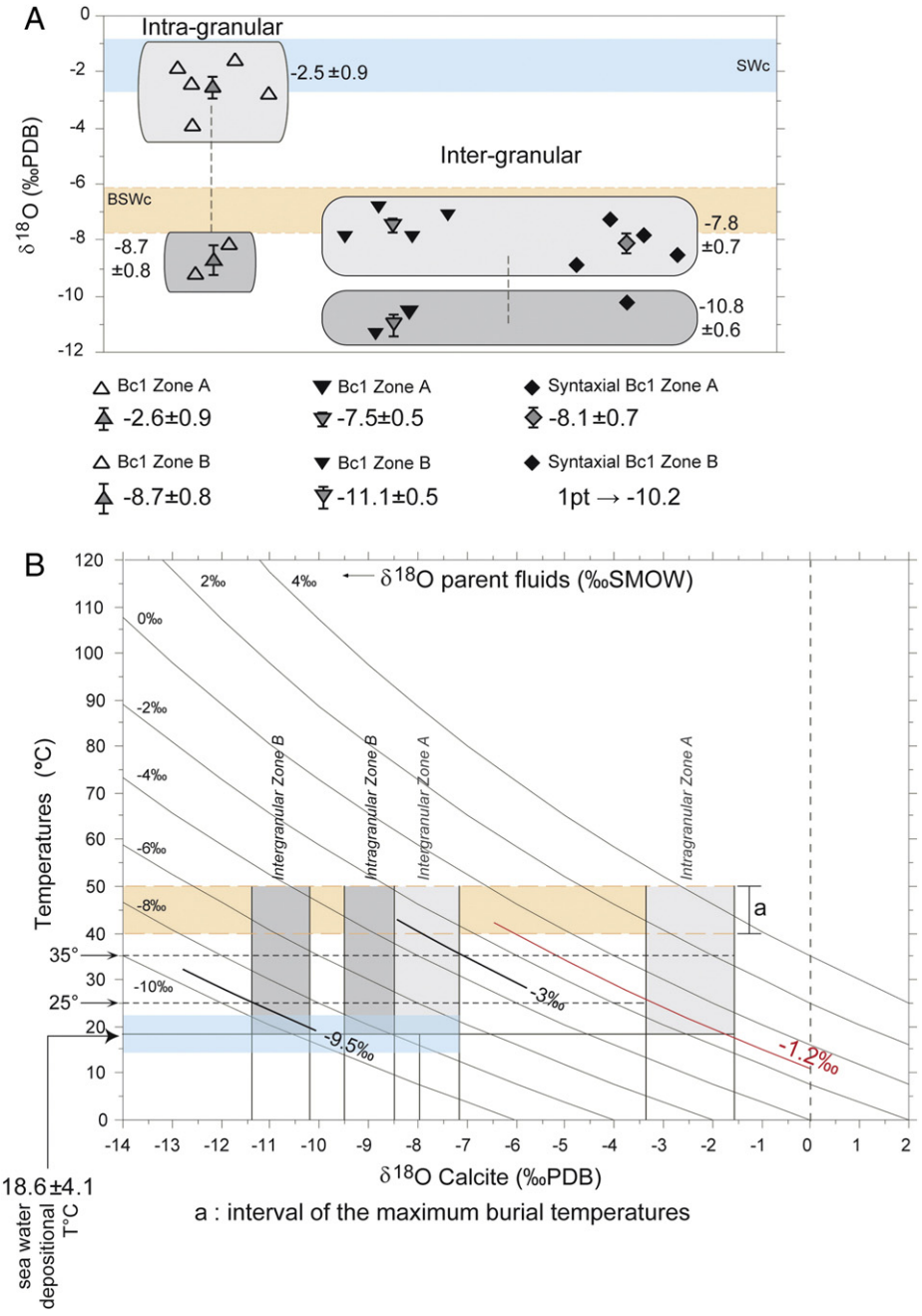

Fig. 8. A- $\delta^{18}O_{PDB}$ of the blocky calcite cements measured on the 2 key SIMS transects (Figs. 4, 5). The CL Zone A of the blocky calcite cement Bc1 displays heavier $\delta^{18}O$ in the intra-particle pore than in the inter-particle pore. The passage from the Zone A to the Zone B records a negative shift towards lighter values, especially in the intra-particle pore (see further discussion in the text). B- Statistic fields (mean ± standard deviation) of the $\delta^{18}O_{PDB}$ of the Bc1 Zone A of inter-particle pore, and Bc1 Zone B of both pores are plotted on a fractionation diagram constructed with the equation of O'Neil et al. (1969). Equilibrium conditions are assumed for the precipitation of these cements contrary to the Bc1 Zone A of the intra-particle pore (see further discussion in the text).

to confirm the possible involvement of biochemical process(es) in the precipitation of the analyzed synsedimentary cement.

A very similar observation is made for the Bc1 blocky calcite cements following the synsedimentary cements in the 2 reference transects performed on the same thin section (Figs. 4, 5). A significant offset is indeed visible between the $\delta^{18}O$ of the first stages of Bc1 cements precipitated respectively in the intra-skeletal pore and the inter-particle pore. In the intra-gastropod pore, the $\delta^{18}O$ of the moderately luminescent Zone A are close to the initial marine calcite values (−2.5‰ ± 0.9; Fig. 8A), whereas the synchronous Zone A in the nearby inter-particle pore displays a lighter $\delta^{18}O$ signature (−7.8‰ ± 0.7; Fig. 8A). The contribution of dissolved aragonite, aragonite dissolution being possibly concomitant to the early blocky calcite cements, could explain the heavier $\delta^{18}O$ of the Zone A of blocky calcite Bc1 in intra-skeletal pores. However, a semi-quantitative compositional map performed on the intra-gastropod pore does not reveal any particularly high Sr content in the Zone A (Fig. 9), which would tend to indicate no or limited contribution of aragonite. It is attractive to propose the

Fig. 9. Electron microprobe semi-quantitative compositional maps of the two key pores (Figs. 4, 5) where SIMS transects were realized. These maps figure the relative distribution of elements in each zone (counts), but do not provide absolute composition. Noteworthy are a strong decrease of Mg content between Bc1 Zone A and Zone B in the intra-particle pore, and a very slight Fe enrichment of the bright orange stripe in the syntaxial overgrowth around the echinoderm debris in the inter-particle pore.

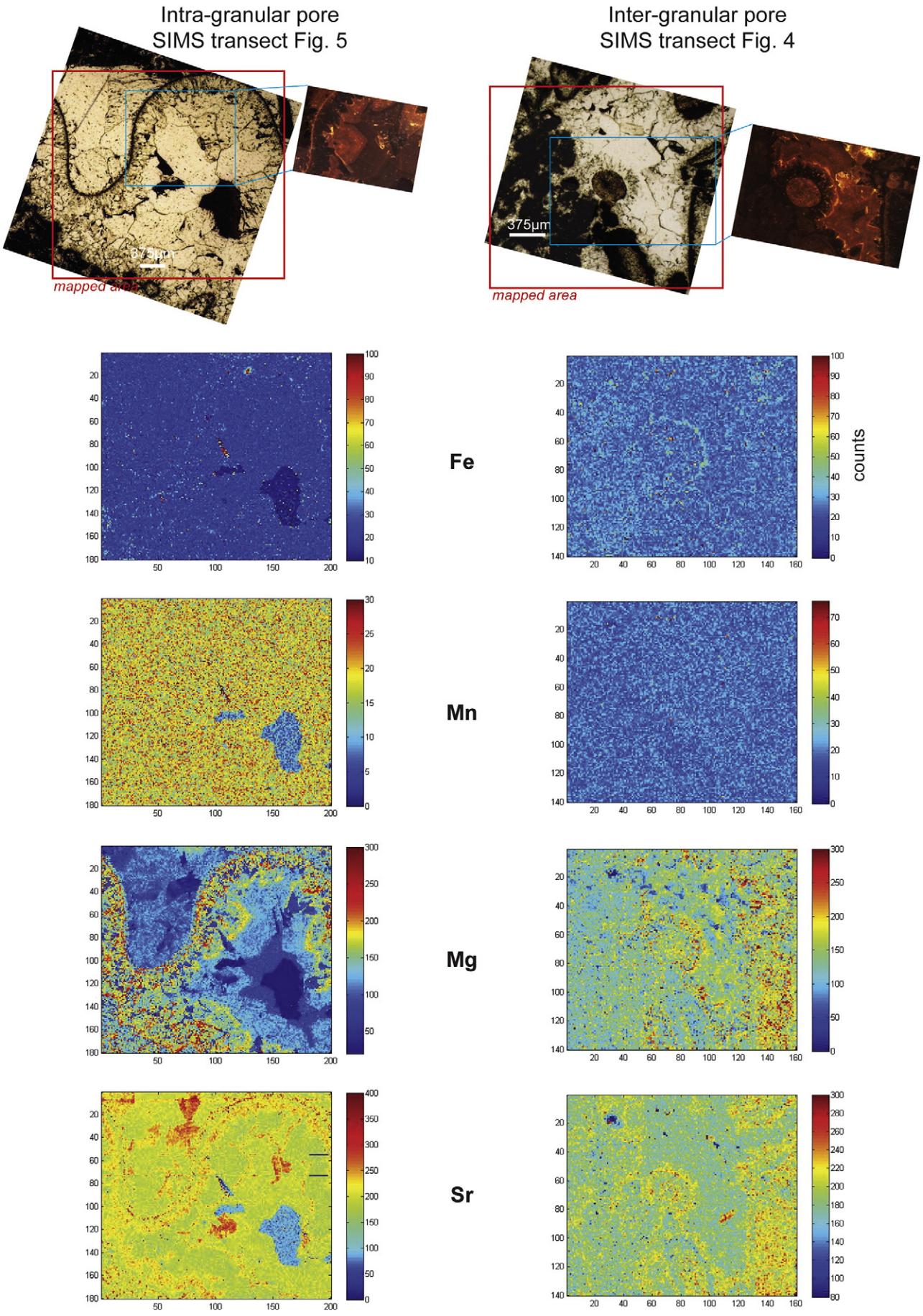
Intra-granular pore
SIMS transect Fig. 5
375µm
mapped area
Inter-granular pore
SIMS transect Fig. 4
375µm
mapped area
Fe
Mn
Mg
Sr
counts

same explanation as for the bladed synsedimentary cement. Indeed, if the microbial catalysis of dissolved carbonate species certainly decreased due to a finite amount of organic matter to be degraded, the control of kinetic effects in the solution on calcite precipitation may have continued, and pH of the water in the intra-skeletal pore remained lower than in the inter-particle pore.

In the inter-particle pore, the passage from Zone A to Zone B within Bc1 cement corresponds to a slight depletion of the $\delta^{18}O$ (from $-7.8‰ \pm 0.7$ to $-10.8‰ \pm 0.6$; Fig. 8A), but marks a stronger shift in the nearby intra-skeletal pore (from $-2.5‰ \pm 0.9$ to $-8.7‰ \pm 0.8$; Fig. 8A). Dickson (1997) demonstrated inter-sectorial isotopic fractionation, but this process cannot explain the huge $\delta^{18}O$ difference observed between Zone A and B. Dickson et al. (1990) reported erratic jumps in isotopic compositions between consecutive CL growth zones, without giving an unequivocal explanation (changes in the nature of pore water and sources of solutes). However, the laser ablation microsampling technique used by Dickson et al. (1990) may have caused erratic thermal fractionation during ablation (*e.g.* Kyser, 1995). In the present study, the jumps are not erratic since they follow the crystal CL zoning pattern. Allison et al. (2010) shown that SIMS $\delta^{18}O$ can be affected by the concentration of other elements compared to conventional mass spectrometer measurement, particularly reporting offsets of 2–3‰ depending on the Sr/Ca ratio. The semi-quantitative compositional map performed on the intra-gastropod pore does not display different Sr concentrations between Zones A and B, but rather illustrates a strong decrease in the Mg content (Fig. 9). Jimenez-Lopez et al. (2004) clearly demonstrated a positive correlation between the Mg concentration in calcite lattice and the $\alpha_{calcite\text{-}water}$. However, the passage from Zone A to Zone B in the inter-particle pore also corresponds to an offset of −3‰, but does not coincide with a significant change in Mg concentration (Fig. 9). Consequently, the shift of $\delta^{18}O$ between the 2 zones of the blocky calcite Bc1 may illustrate a general change in pore water isotopic composition in the inter-particle pore network, synchronous with a homogenization of the chemical conditions of calcite precipitation between inter- and intra-particle pores. A direct physical connection between the different kinds of pores that could be linked to micro-fracturing during burial, a phase reported in the studied carbonates (Vincent et al., 2007), is likely to be at the origin of this overall homogenization of the diagenetic system. Note that within the intra-skeletal pore, the shift in $\delta^{18}O$ may have been emphasized by the more magnesian nature of the Zone A.

Ignoring the values of the Zone A of the Bc1 cement from the intra-skeletal pore, the composition of the parent fluids of these Bc1 cements ranges between $-3.0‰_{SMOW}$ and $-9‰_{SMOW}$ (Fig. 8B). Despite the small scale $\delta^{18}O$ changes revealed by the SIMS, the latter range was used by Vincent et al. (2007) to discuss the timing and nature of large scale fluid flows during burial in Eastern Paris Basin. Indeed, as suggested by Sano et al. (2005) for small scale and large amplitude variations of Mg/Ca in calcites, the revealed isotopic heterogeneities are not necessarily relevant for who those aims are to investigate regional palaeohydrological systems. However; these small scale inter- and intra-crystalline $\delta^{18}O$ heterogeneities are significant and illustrate complex diagenetic systems and patterns. They should be more deeply studied to improve the understanding of high resolution diagenetic processes, and may also help to explain part of the large range of isotopic values that can be classically observed in diagenetic studies involving bulk $\delta^{18}O$ on carbonate cements.

Hoffmann et al. (2016) recently proposed a similar scenario to explain the complex internal structure of belemnite rostra, which involves successively biogenic (biogenically-induced or microbially-induced *sensu* Dupraz et al., 2009) and abiogenic calcite cements filling intra-rostra cavities after post-mortem decay of organic matter. The implications of their results with regard of the use of belemnite rostra as robust proxies for palaeoenvironmental studies find a direct echo here, overall since they claim for the need for high-resolution geochemical analyses to complement their extremely accurate high-resolution petrographic work.

6. Conclusions

The diversity of the oxygen isotope composition of carbonate diagenetic features has been investigated at the highest resolution by the use of SIMS in the Oxfordian shallow-marine carbonates of the Eastern Paris Basin. The $\delta^{18}O$ results obtained from SIMS and classical microdrilling-derived analysis on the same set of products, *i.e.* blocky calcite cements, are similar, but SIMS dataset displays a larger range of values.

Synsedimentary cements are not clear and strong evidence of the original marine isotopic composition because of their high $\delta^{18}O$ variability. HMC-LMC recrystallization may explain part of this range, but more interestingly synsedimentary cements precipitated in intra-skeletal pores show heavier $\delta^{18}O$ than their inter-particle counterparts despite similar petrographical characteristics. The difference in $\delta^{18}O$ between cements within inter- and intra-particle pores is also reported in the first stage of blocky cement growth, intra-skeletal calcites showing heavier $\delta^{18}O$ than the time equivalent and petrographically identical inter-particle calcites. In both kinds of pores, the isotopic evolution shows an overall depletion of the $\delta^{18}O$ from older stage to younger stage of calcite cements, however with significant differences in absolute values and drops between cement CL zones.

The occurrence of micro-diagenetic environments, with distinct oxygen isotopic fractionations, and co-existing at the thin section scale, is tentatively proposed to explain the revealed isotopic offsets. The cause of such differences may be linked to the presence of organic matter in the intra-skeletal pores, implying several microbial processes susceptible to modify strongly the environment during the precipitation of carbonate cements. While the precipitation of synsedimentary cements and early stage of blocky calcite cements occurred under equilibrium condition in inter-particle pores, oxygen isotopic fractionation between calcite and water may have been controlled by kinetic effects in the intra-skeletal pores. In the latter, the pH was probably lowered through a set of microbial process linked to degradation of organic matter, which directly impacted the $\alpha_{calcite\text{-}water}$.

These results may question the sampling strategy for future works. High resolution SIMS analyses reveal a large range of significant small scale heterogeneities in the $\delta^{18}O$ of diagenetic cements. Microdrilling sampling may miss this range of variation, and averaging the values may not necessarily lead to real misinterpretations since this should theoretically render a temperature and/or fluid isotopic composition effect. However, the high amplitude of some of the small scale variations may affect the bulk $\delta^{18}O$ of the carbonate cements. A critical selection of samples is therefore recommended to try to avoid such an effect, like targeting potentially similar micro-diagenetic environments and avoiding potentially specific ones like isolated intra-skeletal grain pores.

Nevertheless, this study also definitely underscore the need for significant additional efforts to be done to improve the reliability of SIMS $\delta^{18}O$ measurements, for instance by better constraining the impact of the variations in major and/or trace element concentrations, in order to develop the use of this very high resolution technique for carbonate diagenesis studies.

Supplementary data to this article can be found online at http://dx.doi.org/10.1016/j.sedgeo.2017.01.008.

Acknowledgements

We would like first to dedicate this work to Jean-Paul Loreau, who left us some years ago, and who initiated this project and more generally developed many research activities in the Dijon University, influencing generations of French carbonate sedimentologists. We gratefully acknowledge M. Chaussidon, E. Deloule, M. Champenois and D. Mangin for the use of the SIMS Cameca 1270. We also thank P. Taubaty for the quality of the thin sections. We thank L.A. Melim, N. Allison, R. Swennen,

T. Dickson, and R. Goldstein for their comments of earlier versions of the manuscript. The authors thank the two reviewers A. Immenhauser and J. Tritlla and the editor B. Jones for their constructive comments that clearly contributed to improve the quality of the final manuscript. A specific thank also to J. Garland for checking the English. This study was supported by a PhD grant from the ANDRA.

References

Aissaoui, D.M., 1988. Magnesian calcite cements and their diagenesis: dissolution and dolomitisation, Mururoa Atoll. Sedimentology 35, 821–841.

Allison, N., Finch, A.A., Webster, J.M., Clague, D.A., 2007. Palaeoenvironmental records from fossil corals: the effects of submarine diagenesis on temperature and climate estimates. Geochimica et Cosmochimica Acta 71, 4693–4703.

Allison, N., Finch, A.A., EIMF, 2010. The potential origin and palaeoenvironmental implications of high temporal resolution $\delta^{18}O$ heterogeneity in coral skeletons. Geochimica et Cosmochimica Acta 74, 5537–5548.

Anderson, T.F., Arthur, M.A., 1983. Stable isotopes of oxygen and carbon and their application to sedimentologic and paleonvironmental problems. In: Arthur, M.A., Anderson, T.F., Kaplan, I.R., Veizer, J., Land, L.S. (Eds.), Stable Isotopes in Sedimentary Geology. Society of Economic Paleontologists and Mineralogists Short Course vol. 10, pp. 1–151.

Blaise, T., Barbarand, J., Kars, M., Ploquin, F., Aubourg, C., Brigaud, B., Cathelineau, M., El Albani, A., Gautheron, C., Izart, A., Janots, D., Michels, R., Pagel, M., Pozzi, J.-P., Boiron, M.-C., Landreain, P., 2014. Reconstruction of low temperatures (<100 °C) burial in sedimentary basins: a comparison of geothermometer in the intracontinental Paris Basin. Marine and Petroleum Geology 53, 71–87.

Brand, U., Logan, A., Hiller, N., Richardson, J., 2003. Geochemistry of modern brachiopods: applications and implications for oceanography and paleocenanography. Chemical Geology 198 (3), 305–334.

Brigaud, B., Puceat, E., Pellenard, P., Vincent, B., Joachimski, M., 2008. Climatic fluctuations and seasonality during the Late Jurassic (Oxfordian-Early Kimmeridgian) inferred from δ18O of Paris Basin oyster shells. Earth and Planetary Science Letters 273, 58–67.

Brigaud, B., Vincent, B., Carpentier, C., Robin, C., Guillocheau, F., Yven, B., Huret, E., 2014. Growth and demise of the Jurassic carbonate platform in the intracratonic Paris Basin (France): interplay of climate change, eustasy and tectonics. Marine and Petroleum Geology 53, 3–29.

Carpentier, C., Lathuiliere, B., Ferry, S., Sausse, J., 2007. Sequence stratigraphy and tectonosedimentary history of the Upper Jurassic of the Eastern Paris Basin (Lower and Middle Oxfordian, northeastern France). Sedimentary Geology 197, 235–266.

Carpentier, C., Lathuilière, B., Ferry, S., 2010. Sequential and climatic framework of the growth and demise of a carbonate platform: implications for the peritidal cycles (Late Jurassic, North-eastern France). Sedimentology 57, 985–1020.

Carpentier, C., Brigaud, B., Blaise, T., Vincent, B., Durlet, C., Boulvais, P., Pagel, M., Hibsch, C., Yven, B., Lach, P., Cathelineau, M., M-C., Boiron, Landreain, P., Buschaert, S., 2014. Impact of basin burial and exhumation on Jurassic carbonates diagenesis on both sides of a thick clay barrier (Paris basin, NE France). Marine and Petroleum Geology 53, 44–70.

Castanier, S., Le Metayer-Levrel, G., Perthuisot, J.P., 1999. Ca-carbonates precipitation and limestone genesis - the microbiogeologist point of view. In: Camoin, G.F. (Ed.), Microbial mediation in carbonate diagenesis. Sedimentary Geology vol. 126, n°1–4, pp. 9–24.

Christ, N., Immenhauser, A., Wood, R., Darwich, K., Niedrmayr, A., 2015. Petrography and environmental controls on the formation of Phanerozoic marine carbonate hardgrounds. Earth-Science Reviews 151, 176–226.

Clermonte, J., Durand, M., Izard, A., Gros, Y., Le Nindre, Y.M., Donsimoni, M., Curial, A., Elion, P., Rebours, H., Vigneron, G., 1998. Site de l'Est - Synthèse des connaissances géologiques; Vol. 1 Texte and Vol. 2 Figures. Technical Report ANDRA, D RP AGEG, pp. 98–287 (152 pp.).

Cox, P.A., Wood, R.A., Dickson, J.A.D., Al Rougha, H.B., Shebl, H., Corbett, P.W.M., 2010. Dynamics of cementation in response to oil charge: evidence from a Cretaceous carbonate field, UAE. Sedimentary Geology 228, 246–254.

De Andrade, V., Vidal, O., Lewin, E., O'brien, P., Agard, P., 2006. Quantification of electron microprobe compositional maps of rock thin sections: an optimized method and examples. Journal of Metamorphic Geology 24, 655–668.

De Wet, C.B., Frey, H.M., Gaswirth, S.B., Mora, C.I., Rahnis, M., Bruno, C.R., 2004. Origin of meter-scale submarine cavities and herringbone calcite cement in a Cambrian microbial reef, Ledger Formation (USA). Journal of Sedimentary Research 74 (6), 914–923.

Debrand-Passard, S., Enay, R., Rioult, M., Cariou, E., Marchand, D., Menot, J.-C., 1980. Jurassique supérieur. In: Mégien, Mégnien (Eds.), Synthèse géologique du Bassin de Paris, volume I "Stratigraphie et paléogéographie". Mémoire du BRGM n°101 (466 pp.).

Dera, G., Brigaud, B., Monna, F., Laffont, R., Pucéat, E., Deconinck, J.-F., Pellenard, P., Joachimski, M.M., Durlet, C., 2011. Climatic ups and downs in a disturbed Jurassic world. Geology 39, 215–218.

Dettman, D.L., Lohmann, K.C., 1995. Microsampling carbonates for stable isotope and minor element analysis; physical separation of samples on a 20 micrometer scale. Journal of Sedimentary Research 65 (3), 566–569.

Deville De Periere, M., Durlet, C., Vennin, E., Lambert, L., Bourillot, R., Caline, B., Poli, E., 2011. Morphometry of micrite particles in Cretaceous microporous limestones of the Middle East: influence on reservoir properties. Marine and Petroleum Geology 28, 1727–1750.

Dhillon, R.S., James, N.P., Kyser, T.K., Bone, Y., 2015. $\delta^{18}O$ and $\delta^{13}C$ variability in brachiopods from modern shelf sediments and its utility for understanding complex oceanography, Southern Australian shelf. Journal of Sedimentary Research 85, 955–967.

Dickson, J.A.D., 1997. Synchronous intracrystalline $\delta^{13}C$ and $\delta^{18}O$ differences in natural calcite crystals. Mineralogical Magazine 61, 243–248.

Dickson, J.A.D., Smalley, P.C., Raheim, A., Stijfhoorn, 1990. Intracrystalline carbon and oxygen isotope variations in calcite revealed by laser microsampling. Geology 18, 809–811.

Dietzel, M., Tang, J., Leis, A., Köhler, S.J., 2009. Oxygen isotopic fractionation during inorganic calcite precipitation-Effects of temperature, precipitation rate and pH. Chemical Geology 268, 107–115.

Dravis, J., 1979. Rapid and widespread generation of recent oolitic hardgrounds on a high energy Bahamian platform, Eleuthera Bank, Bahamas. Journal of Sedimentary Petrology 49 (1), 195–208.

Dupraz, C., Reid, R.P., Braissant, O., Decho, A.W., Norman, R.S., Visscher, P.T., 2009. Processes of carbonate precipitation in modern microbial mats. Earth Science Reviews 96, 141–162.

Elie, M., Landais, P., Fauvel, P.J., 1999. Cinétique de transformation des biomarqueurs pour la détermination de la paléotempérature maximale des sédiments du Callovo-Oxfordien du site de l'Est. ANDRA Scientific Sessions, Atlas des communications par affiche vol. 1 (Abstract book), 15, Nancy 7–9 September 1999.

Frank, T.D., Lohmann, K.C., 1996. Diagenesis of fibrous magnesian calcite marine cement: Implications for the interpretation of $\delta^{18}O$ and $\delta^{13}C$ values of ancient equivalent. Geochimica et Cosmochimica Acta 60 (13), 2427–2436.

Gabitov, R.I., Watson, E.B., Sadekov, A., 2012. Oxygen isotopic fractionation between calcite and fluid as a function of growth rate and temperature: an in situ study. Chemical Geology 306-307, 92–102.

Hendry, J.P., 1993. Calcite cementation during bacterial manganese, iron and sulphate reduction in Jurassic shallow marine carbonates. Sedimentology 40, 87–106.

Hilly, J., Haguenauer, B., 1979. In: Pomerol, Ch. (Ed.), Lorraine – Champagne: *Guides* Géologiques Régionaux. Masson, Paris (216 pp.).

Hoffmann, R., Richter, D.K., Neuser, R.D., Jöns, N., Linzmeier, B.J., Lemanis, R.E., Fusseis, F., Xiao, X., Immenhauser, A., 2016. Evidence for a composite organic-inorganic fabric of belemnite rostra: implications for palaeoceanography and palaeoecology. Sedimentary Geology 341, 203–215.

Humbert, L., 1971. Recherche méthodologique pour la restitution de l'histoire bio-sédimentaire d'un bassin. L'ensemble carbonaté oxfordien de la partie orientale du Bassin de Paris. Nancy University (PhD). (n° AO 5096, 364 pp.).

Ireland, T., 1995. Ion microprobe mass spectrometry: techniques and applications in cosmochemistry, geochemistry, and geochronology. Advances in Analytical Geochemistry 2, 1–118.

Jenkyns, H.C., 2010. Geochemistry of Oceanic Anoxic Events. Geochemistry, Geophysics, Geosystems 11, Q03004. http://dx.doi.org/10.1029/2009GC002788.

Jimenez-Lopez, C., Romanek, C.S., Huertas, F.J., Ohmoto, H., Caballero, E., 2004. Oxygen isotope fractionation in synthetic magnesian calcite. Geochimica et Cosmochimica Acta 68 (16), 3367–3377.

Joachimsky, M.M., 1994. Subaerial exposure and deposition of shallowing upward sequences: evidence from stable isotopes of Purbeckian peritidal carbonates (basal Cretaceous), Swiss and French Jura mountains. Sedimentology 41, 805–824.

Kyser, K.T., 1995. Micro-analytical techniques in stable isotope geochemistry. The Canadian Mineralogist 33, 261–278.

Landais, P., Elie, M., 1999. Utilisation de la géochimie organique pour la détermination du paléoenvironnement et de la paléothermicité dans le Callovo-Oxfordien du site de l'Est de la France. CNRS/ ANDRA Scientific Sessions, Bar-le-Duc, October 1997. EDP Sciences, Paris, pp. 35–58.

Lohmann, K.C., Meyers, W.J., 1977. Microdolomite inclusions in cloudy prismatic calcites: a proposed criterion for former high magnesian calcite. Journal of Sedimentary Petrology 47, 1078–1088.

Martin-Garin, B., Lathuilliere, B., Geister, J., Ramseyer, K., 2010. Oxygen isotopes and climatic controls of Oxfordian coral reefs (Jurassic, Tethys). PALAIOS 25, 721–729.

Mccrea, J.M., 1950. On the isotopic chemistry of carbonates and a paleotemperature scale. Journal of Chemical Physics 18, 849–857.

Moore, C.H., 1989. Carbonate diagenesis and porosity. Developments in Sedimentology vol. 46. Elsevier, Amsterdam (338 pp.).

Morse, J.W., Mackenzie, F.T., 1990. Geochemistry of sedimentary carbonates. Developments in Sedimentology vol. 48. Elsevier, Amsterdam (707 pp.).

Neumeier, U., 1998. Le rôle de l'activité microbienne dans la cimentation précoce des beachrocks (sédiments intertidaux). Terre & Environnement 12 (Genève, 183 pp.).

O'Neil, J.R., Clayton, R.N., Mayeda, T.K., 1969. Oxygen isotope fractionation in divalent metal carbonates. Journal of Chemical Physics 51, 5547–5558.

Riding, R., 2000. Microbial carbonates: the geological record of calcified bacterial-algal mats and biofilms. Sedimentology 47, 179–214.

Riechelmann, D.F.C., Deininger, M., Scholz, D., Riechelmann, S., Schroder-Ritzrau, A., Spotl, C., Richter, D.K., Mangini, A., Immenhauser, A., 2013. Disequilibrium carbon and oxygen isotope fractionation in recent cave calcite: comparison of cave precipitates and model data. Geochimica et Cosmochimica Acta 103, 232–244.

Rollion-Bard, C., Blamart, D., Cuif, J.P., Juillet-Leclerc, A., 2003a. Microanalysis of C and O isotopes of azooxanthellate and zooxanthellate corals by ion microprobe. Coral Reefs 22, 405–415.

Rollion-Bard, C., Chaussidon, M., France-Lanord, C., 2003b. pH control on oxygen isotopic composition of symbiotic corals. Earth and Planetary Science Letters 215, 275–288.

Rollion-Bard, C., Erez, J., Zilberman, T., 2008. Intra-shell oxygen isotope ratios in the benthic foraminifera genus Amphistegina and the influence of seawater carbonate chemistry and temperature on this ratio. Geochimica et Cosmochimica Acta 72, 6006–6014.

Sano, Y., Shirai, K., Takahata, N., et al., 2005. Nano-SIMS analysis of Mg, Sr, Ba, and U in natural calcium carbonate. Analytical Sciences 21 (9), 1091–1097.

Sass, E., Bein, A., Almogi-Labin, A., 1991. Oxygen-isotope composition of diagenetic calcite in organic-rich rocks: evidence for 18O depletion in marine anaerobic pore water. Geology 19, 839–842.
Sellwood, B.W., Shepard, T.J., Evans, M.R., James, B., 1989. Origin of late cements in oolitic reservoir facies: a fluid inclusions and isotopic study (Mid-Jurassic, southern England). Sedimentary Geology 61, 223–237.
Shackleton, N.J., Kennet, J.P., 1975. Palaeotemperature history of the Cenozoic and the initiation of Antartic glaciation – Oxygen isotope analyses in DSDP sites 277, 279 and 281. Initial Report DSDP 29 pp. 743–745.
Smalley, P.C., Stijfhoorn, D.E., Raheim, A., Johansen, H., Dickson, J.A.D., 1989. The laser microprobe and its application to the study of C and O isotopes in calcite and aragonite. Sedimentary Geology 65, 211–221.
Swart, P.K., Burns, S.J., Leder, J.J., 1991. Fractionation of the stable isotopes of oxygen and carbon in carbon-dioxide during reaction of calcite with phosphoric acid as a function of temperature and technique. Chemical Geology 52, 365–374.
Tucker, M.E., Wright, V.P., 1990. Carbonate Sedimentology. Blackwell, Oxford (482 pp.).
Veizer, J., 1983. Trace elements and isotopes in sedimentary carbonates. In: Reeder, R.J. (Ed.), Carbonates: mineralogy and chemistry. Reviews in Mineralogy 11, p. 265 (299).
Vincent, B., 2001. Sédimentologie et géochimie de la diagenèse des carbonates. Application au Malm de la bordure Est du Bassin de Paris. University of Burgundy (Ph.D. Thesis). (308 pp.).
Vincent, B., Emmanuel, L., Houel, P., Loreau, J.P., 2007. Geodynamic control on carbonate diagenesis: petrographic and isotopic investigation of the Upper Jurassic formations of the Paris Basin (France). Sedimentary Geology 197, 267–289.